Suspended False Ceiling acoustic elements theoretical and experimental investigation

[1] Giovanni Amadasi, [2, 3] Franc Policardi-Antoncich
[1] *Vibro-Acoustic SCS & Partners, Via Antoniana 278, 35011 Campodarsego PD, Italy*
[2] *LUCAMI, Fakulteta za elektrotehniko, Tržaška cesta 25, SI-1000 Ljubljana, Slovenija*
[3] *Raziskovalni Inštitut za nove tehnologije in energetiko (R.I.N.T.E.) d.o.o., Stritarjeva 6/a, 4000 Kranj, Slovenia*
g.m.amadasi@scs-controlsys.com

Abstract

This research work investigates the all-together sound package alphacell® software used for Suspended False Ceiling acoustic elements (SFCae), in order to understand the influence of Panel Perforation (PP) and the porous characteristics on Sound Absorption (SA) values. The present study investigates the poro-acoustic materials physical models of each layer and the theoretically achieved results for the multi-layers, by varying and optimizing the physical model parameters of Porosity and Flow-Resistivity. More than 20 standard perforation patterns were also experimentally investigated, confirming the theoretically obtained results. The present paper deals with 14 standard perforation patterns.

1 Introduction

Suspended False Ceiling acoustic elements (SFCae) are widely used in closed spaces to correct room acoustics. They present different layers and surface finishings; their acoustic performance is normally expressed with only an overall absoption coefficient α_W, which does not always represent the real acoustic characteristics of the ceiling. The hypothesis of the present study is that most of the published data are just consequence of specific installation results mixed with ISO 354:2003 and/or ISO 10848-2:2006 standard test procedures. The mentioned standards' results are affected by test methods boundary conditions and these results can not be used "as they are" for room acoustic design and simulation.
Many existing standard products and solutions on the market were investigated and tested using: A) a SCS-9020B© Impedance tube compliant with ISO 10534-2 for Normal incidence (plane waves) α_N coefficient, B) a SCS-9031© small reverberation chamber tuned to match ISO 354 for diffuse field giving the α_{Stat} coefficient and C) a Flow-Resistivity testing device SCS-9023© complying with ISO 29053-2.
The experimental results have been compared to the physical models simulated by the *alphacell®* software (TIMM method), in order to reach a suitable agreement between experimental results and physical model choices. Analysis and optimization processes were conducted varying the characteristic parameters of every single layer using the *alphacell®* [1] software, investigating the presented results.

2 Parameters Definition

Most of the results were theoretically achieved for the multi-layers combination by varying and optimizing the poro-acoustic materials physical model parameters Porosity and Flow-Resistivity on the one side, and by changing the holes geometrical characteristics of the Perforated Panels "PP" on the other side.

2.1 Open Porosity

Open Porosity (ϕ in %) is the ratio between the interconnected void volume and the total volume of a material. The theory states that it is enough to measure the volume vs. mass ratio of an absorber sample, but in real conditions this parameter is difficult to measure because: a) in case of open cell foams it is hard to determine which cells are really open and interconnected, b) in case of fibrous absorbers it is difficult to measure the exact volume of a compressible sample. Just as a general example, poro-acoustic materials achieve up to 95-98% of ϕ for fibrous absorbers. One simple method to measure ϕ consists of filling the sample pores with a liquid and measure its volume, but the liquid can contaminate the sample and preclude other parameter measurements. Another method uses thermodynamics: the sample is placed in a chamber which is compressed, leading to a volume differential ΔV, so the internal pressure will increase by ΔP according to Boyles law:

$$V_0 + V_t = -\frac{P_0 + \Delta P}{\Delta P}\Delta V \tag{1}$$

2.2 Static air flow resistivity

Static air flow resistivity (σ) (N.s.m−4), also called Resistivity, it is defined as: $\sigma\phi\vec{v} = -\vec{\nabla} p$, an expression representing the generalized Darcy's law in which ϕ is the open porosity of the material, $\vec{v}$ the velocity of the fluid particles subjected to the pressure gradient $\vec{\nabla}p$, and $\phi\vec{v}$ is the fluid flow inside the porous material.
The definition of σ is based on the assumption that $\vec{v}$ and $\vec{\nabla} p$ are constants (Static Resistivity). Some authors prefer to use the static viscous permeability k_0 instead of the static air-flow resistivity. The static permeability, expressed in m^2, is defined as $k_0=\eta\sigma$, where η is the dynamic viscosity of air (~1.84 × 10−5 N.s.m−2 at normal temperature and pressure conditions). It should be pointed out that k_0 does not depend on the fluid property, whereas σ does.

σ represents the visco-inertial effects at low frequencies (viscous boundary layer of the same order of magnitude of the characteristic pore size). The Delany-Bazley and Delany-Bazley-Miki physical models [2] use only this parameter to describe the behavior of fibrous acoustical materials. σ values in poro-acoustical materials spans between 10^3 and 10^6 N.s.m−4.

2.3 Transparency Index

Transparency Index (TI) considers a perforated plate as a porous material using macroscopic parameters. The two extremes 10% open area surfaces are either making a single large hole in the center or making very fine perforations overall the surface. In the first case, instead of a transparent facing material, there is a small completely open area at the surface center and the rest is completely opaque to sound reflecting all of it. In the second case, the entire surface is almost completely transparent to sound, because the tiny solid areas between the holes are too small to interact with the sound waves. TI index was introduced by Schultz [3] and is defined by the following formula:

$$TI = nd^2/ta^2 = 0.04\ P/\pi ta^2 \quad (2)$$

Where:
n = number of perforations per square inch (in^{-2});
d = perforation diameter (in);
t = sheet thickness (in);
a = shortest distance between holes (in);
a = b – d, where
b = on-center hole spacing (in);
P = percent (not fractional) surface open area.

Acording to the Delany-Bazley-Miki physical model [2], the open porosity ϕ determines the sound attenuation i.e. the perforated plate screen effect, becoming more important at high frequencies. Figure 1 shows the attenuation at 10kHz as a function of TI.

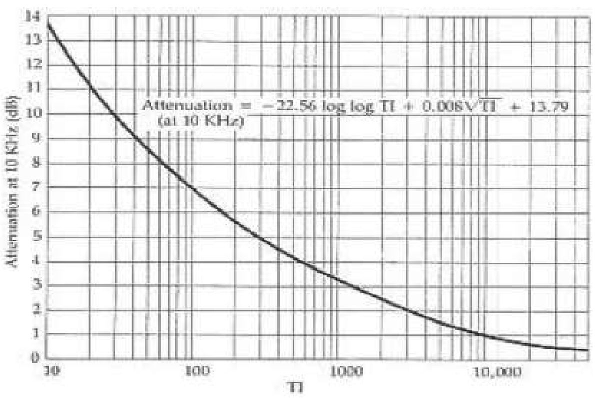

Figure 1. TI index: Schultz graph attenuation at 10kHz

Table 1 shows a comparison between two different PP with an 8x TI index difference (PP1 11.562, PP2 1.439), in which the sound attenuation at 10kHz drops from 2.83 down to 0.91 dB.

Table 1. Strong TI index difference in two perforated plates

Parameter	sample 1	sample 2
	mm	mm
n = number of perforations per sq in; n = 1/A	396,9100	73,6700
d = perforation diameter	0,5800	1,6700
t = sheet thickness	0,4700	1,5900
a = shortest distance between holes; a = b – d	0,0311	0,0594
b = on-center hole spacing	1,3700	3,1800
A = sheet area per hole = b^2cos 30^0	0,0025	0,0136
angle degree °	30,0000	30,0000
P % open area - Porosity = [(pd^2/4)/A] x 100	16,2400	24,9900
TI = nd2/ta2	11.562,00	1.439,000
Attenuation at 10 kHz = -22.56 log log TI + 0.008vTI + 13.79dB	0,9100	2,8300

3 Simulation models validation

The *alphacell®* software can compute the acoustic behavior of very different systems, as for example those composed by air-gaps, isotropic & orthotropic solids and isotropic porous media. It uses Delany-Bazley-Miki, Hamet, Attenborough, and Johnson-Champoux-Allard-Pride-Lafarge models. The software takes into account the material's Pore Size Distribution (PSD), Micro-Perforated Panels (MPP) with circular, rectangular or slit-like perforations also, and it is suitable for Woven and Non-Woven textiles too.

alphacell® is capable to apply the model developped by Biot in 1956 [4], [5] to all previous acoustic models, in order to include the elastic effects of the porous frame as: visco-elastic isotropic, limp and rigid body behaviour, heavy-layer like, impervious screen and the double porosity by Olny & Boutin [6]. The software can compute multi-layered structure acoustic responses with arbitrary incidence plane waves, modal sound field, diffuse sound field, mechanical force, turbulent boundary layers and even rain on the roof and many more.

Experimental data from different PP (PP1 to PP7) were extracted using the Kundt impedance tube as in A) and the Flow-Resistance device as in C). The validation procedure compared all the experimental data as in B) for every PP sample with software simulation results. The layers sequence model used in the the Kundt tube consists of a PP, a TNT thin tissue and an air gap. This last one was generally chosen 200 mm as it is the distance between the inner face of the TNT tissue and the Kundt tube end. The TNT tissue thickness was kept constant between 0.2/0.25mm and the variables were 1) the PP perforation characteristics and 2) the PP thickness.

Different PP were chosen from the normal industrial production in order to represent a broadband spectrum of the available SFCae.

3.1 Normal incidence sound wave: real data vs. simulation data

Sound waves expansion in a free or semi-free field is practically spherical. Interactions between sound waves in free air and a ceiling are strongly influenced by their incidence planes. These are are theoretically infinite, but in order to achieve a suitable comprehension, sound wave incidence planes are studied for normal (90°) incidence and for approximized random incidence planes named Diffuse Field.

Table 2 shows the holes geometric data for all the PP samples; circular perforation is the common one, representing 6 of the 7 samples, while only 1 sample is made with square holes. The number of perforations spans from a minimum of 14,26 up to 101,38 holes /sq. inch. Hole dimensions are also very different, spanning from 0,75 up to 4 mm, with a variability more than 5 x, so that TI values span between a minimum of 34 up to 824.

Parameter / Comments		PP 1	PP 2	PP 3	PP 4	PP 5	PP 6	PP 7
Perforation C=circular, Sq=squared		C	C	Sq	C	C	C	C
n = number of perforations per sq in; n = 1/A		25.34	36.50	14.26	25.81	101.38	36.50	74.48
d = perforation diameter	mm	2.50	2.00	4.00	0.75	1.00	2.00	2.00
t = sheet thickness	mm	0.70	0.60	0.60	0.60	0.50	0.50	5.00
a = shortest distance between holes: a = b – d	mm	0.1378	0.1181	0.1575	0.1673	0.0787	0.1181	0.0591
b = on-center hole spacing	mm	6.00	5.00	8.00	5.00	3.00	5.00	3.50
A = sheet area par hole = $b^2 \cos 30^0$	mm2	0.0395	0.0274	0.0701	0.0388	0.0099	0.0274	0.0134
angle deg	deg	45.00	45.0	45.0	-	45.0	45.0	45.0
P % open area - Porosity= $[(pd^2/4)/A] \times 100$	%	19.2736	17.7625	27.7539	1.7663	12.3351	17.7625	36.2500
TI = nd2/ta2		469.20	686.66	603.51	34.02	1 287.49	823.99	672.65
Attenuation at 10 kHz = - 22.56 log log TI + 0.008vTI + 13.79	dB	4.34	3.78	3.97	9.66	2.96	3.53	3.81

Table 2. 7 PP samples hole geometry data

Table 3 shows Flow Resistivity "r" data for all PP samples; sample thickness is almost the same, the measured r values range from 4.962 up to 8.329 and the RS Specific r ranges from 38,95 up to 65,38. r ranges from a minimum of 7.790 up to a huge 128.395, with a 16,5x difference factor.

Parameter	Comments		PP 1	PP 2	PP 3	PP 4	PP 5	PP 6	PP 7
d sample	thikness	mm	0.70	0.60	0.60	0.60	0.50	0.50	0.50
R (measured)	Dp/Qv	Pa s/m^3	6 022	6579	8 190	8 329	8 178	6 414	4 962
Dp	diff. Pa (mic.)	Pa	23.64	25.82	32.15	32.69	32.10	25.17	19.48
Qv	Volume flow	m^3/s	3.93E-03						
Rs Specific R	R A = Dp/v	Pa s/m	47.27	51.65	64.29	65.38	64.20	50.35	38.95
v	air speed	m/s	0.5						
A	Sample Area	m^2	0.00785						
r Flow Resistivity	Rs/d = Dp/(v d) (Ns/m4)	Pa s /m^2	67 532	86 075	107153	108971	128395	100700	7790

Table 3. 7 PP samples Flow Resistivity "r" data

Table 4 shows r data for all PP samples but with an added TNT layer; sample thickness remains the same. The measured r values range from 38.140 up to 63.070, and the RS Specific r ranges from 299,40 up to 495,1 both with an enormous increase from Table 3. The difference with/without TNT spans from 65.089 up to 737.994 i.e. more than 11 times.

Parameter	Comments		PP1 + TNT	PP2+ TNT	PP3 + TNT	PP4 + TNT	PP5 + TNT	PP6 + TNT	PP7 + TNT
d sample	thikness	mm	0.70	0.60	0.60	0.60	0.50	0.50	0.50
R (measured)	Dp/Qv	Pa s/m^3	38 140	49190	63070	44 520	52 020	53 420	46 420
Dp	diff. Pa (mic.)	Pa	149.70	193.1	247.6	174.7	204.2	209.7	182.2
Qv	Volume flow	m^3/s	3.93E-03						
Rs Specific R	R A = Dp/v	Pa s/m	299.40	386.1	495.1	349.5	408.4	419.4	364.4
v	air speed	m/s	0.5						
r F. Resistivity	Rs/d = Dp/(v d) (Ns/m4)	Pa s /m^2	427713	643569	825166	582470	816714	838694	72879
Difference w/out TNT			360180	557494	718013	473499	688319	737994	65 089

Table 4. 7 PP samples + TNT Flow Resistivity "r" data

After the PP complete objective analysis and measurement, a model validation was performed, based on Impedance tube results for α_N coefficient and *alphacell*® software on PP1 and on PP4 for the normal incidence plane. The comparison was performed in 1/3 octave bands from 50 Hz up to 1.5 kHz and the showed tolerances are quite acceptable for acoustic modeling.

Figure 2 verifies PP1 + TNT ϕ = 19% with σ 360 kPa s/m^2 and the compliance is very good or at least good in all frequency bands, with slight differences in the upper frequency bands.

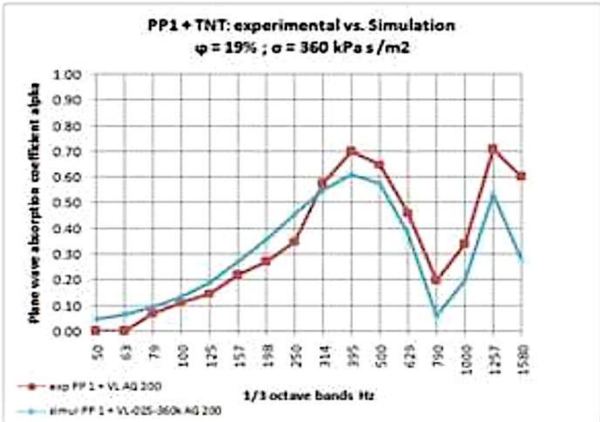

Figure 2. PP1 + TNT experimental vs. simulation

Figure 3 verifies PP4 + TNT ϕ = 1,8% with σ 580 kPa s/m^2 and the compliance is very good or at least good in all frequency bands, with slight differences in the lowest frequency band.

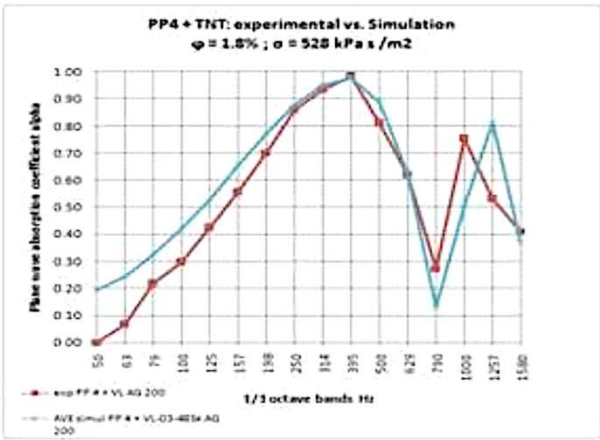

Figure 3. PP4 + TNT experimental vs. simulation

3.2 Diffuse field incidence sound wave: real data vs. simulation

As already mentioned, a complete sound wave incidence study must take into account the almost infinite random non α_N normal incidence planes named α_{Stat} Diffuse Field. In this situation sound waves bounce the surface from multiple statistically random non defined planes, interacting with the surface and in this case with its holes in a different way.

Figure 4 shows how the random α_{Stat} Diffuse Field incidence planes differs from the α_N normal incidence plane, with a significant sound absorption drop in a PPx sample (any sample with ϕ >12%) + TNT and PP4 + TNT.

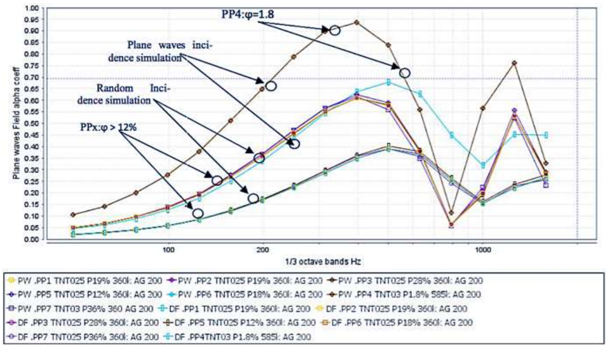

Figure 4. α_N normal incidence plane and α_{Stat} Diffuse Field simulation for a PPx sample (any sample with ϕ >12%) + TNT and PP4 + TNT of 1,8 %

The simulation was then extended up to 5 kHz (Figure 5) for a PPx sample (any sample with ϕ >12%) and PP4 (ϕ = 1.8%), both for Plane waves "PW" and Random incidence α_{Stat} Diffuse Field conditions.

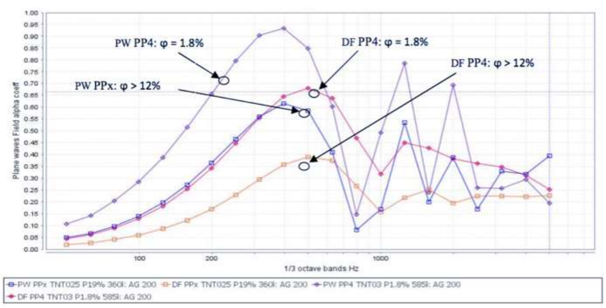

Figure 5. α_N normal incidence plane and α_{Stat} Diffuse Field simulation for a PPx sample (any sample with ϕ >12%) + TNT and PP4 + TNT with ϕ 1,8 % extendet do 5 kHz

The simulation substantially confirmed the PP + TNT behaviour.

4 Conclusion

After the experimental validation of the model simulation, it has been shown how it is possible to study multi-layers in order to correctly design a Suspended False Ceiling acoustic element SFCae through a specific software.

The simulation studied the holes diameter optimisation by applying *alphacell®* features to PP at first instance by considering geometry parameters (D and φ) and estimating the α_{Stat} up to 5 kHz.

The simulation took into account the Plate tickness, the holes diameters at constant porosity, the Flow Resistivity and the Open Porosity in order to maximize the sound absorption whith a the specific air flow resistance adding TNT tissue obtaining a significant sound absorption as well as a full spectrum good balance absorption.

This paper also demonstrate that to some extent the single-number rating α_W EN ISO 11654, based on the limited frequency interval 250 - 4.000 Hz, does not provide sufficient information to acousticians and it does not take into account the balance of α_{Stat} Diffuse Field in the full spectrum range.

Aknowledgements

The authors wish to acknowledge the precious help of Atena Spa for the PP samples and the TNT tissues, Matelys research raboratory for the scientific support and bright ideas in using *alphacell®* software, SCS-Euroacoustic laboratory for experimental test on porous materials, R.I.N.T.E. and LUCAMI for DOE and present paper writing.

References

[1] alphacell.matelys.com, 10. 7. 2020

[2] Delany M. E. and Bazley E. N., Acoustical properties of fibrous absorbent materials, Applied Acoustics 3, 1970, pp. 105-116, DOI: 10.1016/0003-682X(70)90031-9

[3] Theodore J. Schultz, Acoustical uses for perforated metals, Ph.D. dissertation, Houston - Texas, 1986

[4] M. A. Biot, *Theory of propagation of elastic waves in a fluid saturated porous solid. I Low frequency range*, J. Acoust. Soc. Am. 28, pp. 168–178, 1956

[5] M. A. Biot, *Theory of propagation of elastic waves in a fluid saturated porous solid. II Higher frequency range*, J. Acoust. Soc. Am. 28, pp. 179–191, 1956

[6] X. Olny, C. Boutin, Acoustic wave propagation in double porosity media, The Journal of the Acoustical Society of America 114, 73 (2003)